



Effect of composition on the polarization and ohmic resistances of LSM/YSZ composite cathodes in solid oxide fuel cell

B SHRI PRAKASH*, S SENTHIL KUMAR and S T ARUNA

Surface Engineering Division, Council of Scientific and Industrial Research-National Aerospace Laboratories, Bangalore 560 017, India

*Author for correspondence (spbadi@nal.res.in)

MS received 4 August 2016; accepted 24 March 2017; published online 9 June 2017

Abstract. $\text{La}_{0.8}\text{Sr}_{0.2}\text{MnO}_{3-\delta}$ (LSM)/8 mol% yttria-stabilized ZrO_2 (YSZ) (LSM/YSZ) composite cathodes with varying composition are studied for both polarization and ohmic resistance by electrochemical impedance spectroscopy. It was found that total resistance and polarization resistance are lowest for the composite with 60 wt% of LSM (LSM60/YSZ40). However, the ohmic resistance was highest for the same composition and amounted to 60% of the total resistance value. Compositional dependence of resistances has been explained based on the variations of the triple phase boundaries and width of the O^{2-} ion migration path with the composition of the electrode. Based on the observed area specific ohmic resistance values for the composite cathodes, it is proposed to verify the advantages of LSM/YSZ over LSM cathode in anode-supported solid oxide fuel cell with thin electrolyte.

Keywords. Solid oxide fuel cell; composite cathodes; polarization resistance; ohmic resistance; impedance spectroscopy.

1. Introduction

In electrolyte-supported solid oxide fuel cell (SOFC) or in anode-supported SOFC with thick film electrolytes ($>50\ \mu\text{m}$), ohmic resistance originating from electrolytes dominates and becomes the major source of the performance loss. In the recent times, in the anode-supported SOFC, by depositing very thin ($<10\ \mu\text{m}$) and/or high conducting electrolytes, ohmic losses from the electrolytes has been brought down to a level that focus has now shifted to the cathode, which is the next major source of voltage loss [1–4].

$\text{La}_{1-x}\text{Sr}_x\text{MnO}_{3-\delta}$ (LSM) is the most commonly used cathode material in high temperature SOFC (HT-SOFC), as it has good electrochemical activity for the O_2 reduction reaction (ORR) at high temperatures, good thermal, structural and chemical stabilities. Its compatibility with the commonly used electrolytes: 8 mol% yttria-stabilized zirconia (YSZ) and gadolinia-doped ceria (GDC) is also excellent [5]. LSM is a good electronic conductor ($\sigma_e \sim 200\ \text{S cm}^{-1}$ at 800°C) [6], but with a negligible oxygen ionic conductivity ($\sim 4 \times 10^{-8}\ \text{S cm}^{-1}$) and low oxygen surface exchange coefficient [7,8]. As the incorporation and bulk diffusion of oxygen ion inside LSM cannot be expected to occur to a significant degree, ORR is limited to triple phase boundary (TPB) areas at the electrode/electrolyte interface (figure 1a).

With the limited number of TPB's at the electrode/electrolyte interfaces, area specific resistance (ASR) or polarization resistance (R_p) as high as $>100\ \Omega\ \text{cm}^2$ has been reported for pure LSM at 800°C [9]. One of the strategies to improve the performances of LSM-like pure electronically conducting

cathodes is through the addition of ionic conducting phases such as YSZ and GDC [10–16]. Decreased R_p results from the extension of electrochemical reaction into the bulk of the cathode electrode and increase in the number of TPB's.

ORR in LSM or LSM/YSZ composite is believed to occur through following steps: (i) surface adsorption of O_2 and dissociation on LSM (O_{ad}), (ii) surface diffusion of O_{ad} on LSM, (iii) conversion of O_{ad} into oxygen ion (O^{2-}) by the charge transfer reaction from the electrons (e') flowing through the LSM and subsequent incorporation of O^{2-} into YSZ lattice at TPB and (iv) O^{2-} transport in YSZ lattice (figure 1a) [17]. Conversion of electronic current (e' current) into ionic current (O^{2-} current), thus occurs through multi-step phenomenon. In the case of pure LSM, O^{2-} formed at the TPB's directly enters into the dense YSZ lattice of the electrolytes (figure 1a). On the other hand, in LSM/YSZ composite cathodes, prior to entering into the dense electrolyte (electrolyte–electrolyte), O^{2-} ions need to flow through the low temperature sintered ($\sim 1150^\circ\text{C}$) YSZ sub-lattice (electrode–electrolyte) of the cathode (figure 1b).

The advantage of LSM/YSZ composite cathode over LSM cathode has been extensively investigated with studies primarily focussing on the influence of composition on the R_p . As in the case of polymer composites, composite cathode also depend on many factors such as composition, particle size, etc. [18–20]. Based on the experimental investigations and theoretical models, it has been shown that composition, particle size, particle size ratio and firing temperature are the important factors which influence the

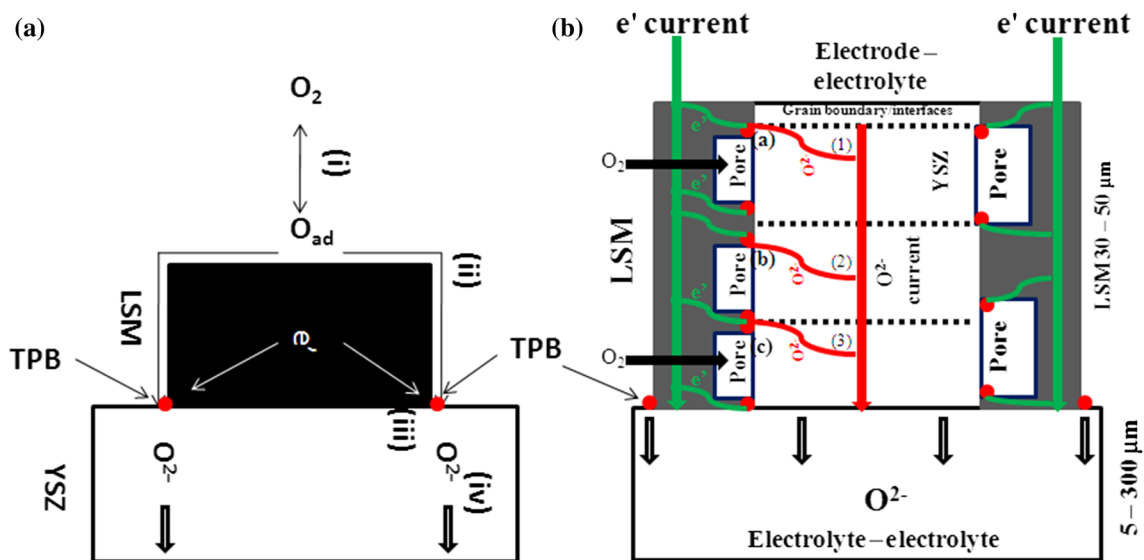


Figure 1. Schematic diagrams showing the location of the TPB and the conversion of electronic current into ionic, while using (a) LSM and (b) LSM/YSZ as cathode on YSZ electrolyte.

TPB and in turn R_p [14,21–27]. Maximization of TPB sites has been reported to be essential to minimize the R_p of the cathodes. Armed with advanced characterization techniques such as focussed ion beam-scanning electron microscopy (FIB-SEM), full-field transmission X-ray microscopy, etc., reports can be found in the literature discussing the variation of the TPB with cathode composition and its effects on the R_p and overall performance of the cell [13,14,28,29]. For LSM and YSZ powders with equisized particles, based on both modelling and experimental studies, it has been shown that 50–50 wt% is optimum composition to achieve minimum R_p and maximum performance, where connectivity between two solid phases can be expected to be highest [14]. Accordingly, most of the LSM/YSZ studies have focussed on cathodes with ~50 wt% YSZ. However, in the literature, variable values for optimum composition can also be found. Optimum composition might shift to the higher/lower wt% of LSM, if LSM powders with higher/lower particle sizes are used [13,30]. Though LSM/YSZ composite cathodes with superior performance have been demonstrated, for further lowering of the resistance, it is necessary to decode the cathode resistances and ascribe it to a definitive fundamental mechanisms involved in ORR. In addition to the R_p , it is also necessary to give importance to the ohmic resistance originating from the cathode.

Virkar *et al* [31] employed *in situ* current interruption technique to measure the ohmic resistance of the cathode interlayer (50 wt% of LSM) fired at 1200°C by varying its thickness and keeping thickness and other parameters of the remaining components constant. They observed a linear relation between the resistance and the thickness of the interlayer with an associated resistivity of 3.92 Ω cm at 800°C.

High resistivity observed for LSM/YSZ composite in comparison to pure LSM ($5 \times 10^{-3} \Omega$ cm) is in accordance with the higher volume fraction of the insulating phases (~60% (porosity + YSZ)) in the composite. However, linear dependence of the cathode ohmic resistance with thickness is bit surprising.

To the best of authors knowledge, studies on the ohmic resistance (R_{ohmic}) variation of the composite cathode with the composition are scanty or nil. While using pure LSM as cathode, irrespective of the thickness of the cathode layer, conversion of e' current into O^{2-} current takes place only at the TPB sites of electrode/electrolyte interface area (represented by red circles in the figure 1a). Since electronic conduction in LSM (~ 200 S cm^{-1} at 800°C) is much higher than the ionic conduction in YSZ (~ 0.04 S cm^{-1} at 800°C), ohmic resistance measured across the cell would mostly equal to the electrolyte resistance. In such cases Ohmic resistance measured across the cell can be entirely attributed to the electrolyte by ensuring the good contact between electrode and current collector (minimum contact resistance) and by separating the current and voltage measurement probes.

While using LSM/YSZ composite as cathodes, as shown in figure 1b, conversion of e' current into the O^{2-} current can occur either close to the interface or far away from it. If it is presumed that electrochemical reaction occurs at a point far away from electrode/electrolyte interface (point (a)) of LSM/YSZ composite (figure 1b), charge travels through most of the electrode region as an ionic species (path (1)), and in the electrodes with 50 μm thickness, ion travels an additional $\sim 50 \mu m$ distance before entering into dense electrolyte. Resistance for e' current in LSM can be assumed to be negligible (when compared to ionic resistance in YSZ),

whereas resistance for O^{2-} current in the electrolyte part of the electrode would be substantial, as ions have to move through the YSZ component which has been fired at substantially lower temperature ($\sim 1200^\circ\text{C}$) than its actual sintering temperature ($> 1400^\circ\text{C}$). In such a scenario, ions have to travel through high resistive grain boundaries/interfaces and need to face constriction effects at the grain–grain interfaces. Hence, effective resistivity for ionic conduction in electrolyte component (YSZ phase) of the electrode would be much higher than the actual electrolyte, which has been sintered at high temperature to attain full densification ($\rho \sim 25 \Omega \text{ cm}$ at 800°C). It has been reported in the literature that YSZ networks in LSM/YSZ composites has an effective oxygen-ion conductivity which is significantly lower than the expected values on the basis of volume fraction of non-ionic conducting regions (LSM + pores). This is due to the network interruptions and/or constriction effects [32]. In such a scenario, overall ohmic resistance from a cathode half cell can be expected to be much higher than the resistance emanating from the electrolyte alone. The present investigation mainly focusses on the measurement of the variation of the R_{ohmic} along with R_p of LSM/YSZ composite cathode with composition. Through this paper, we are insisting that variation in ohmic resistance should also be given a due importance alongside changes in R_p with variation in composition.

2. Experimental

Electrolyte membranes were fabricated through a non-aqueous tape casting method using 8 mol% yttria-stabilized zirconia (8YSZ, Tosoh). Green layers were sintered at 1400°C per 4 h to obtain dense membranes. Sintered electrolytes had the dimension of $\sim 300 \mu\text{m}$ thickness and $\sim 20 \text{ mm}$ in diameter. In addition, few thicker pellets of electrolytes ($\sim 2 \text{ mm}$) were also fabricated by conventional pressing and sintering.

LSM/YSZ composite powder was prepared by ball milling the mixture of commercially procured $\text{La}_{0.8}\text{Sr}_{0.2}\text{MnO}_{3-\delta}$ powder (Nextech) and Tosoh YSZ powder in distilled water for 5 h followed by drying in oven at 150°C . Particle size analysis of both the powders was performed after milling the individual powder for the duration equal to the time of milling employed for LSM/YSZ composite preparation, using laser light scattering method (Mastersizer 2000, Malvern Instruments). Particle size analysis was performed on milled LSM/YSZ composite powder also.

Composition of LSM/YSZ was varied from 100 to 40 wt% of LSM and hereafter would be referred as L100/Y0 (pure LSM) to L40/Y60 (40 wt% of LSM and 60 wt% of YSZ), respectively. Cathode paste/ink was prepared by thoroughly mixing LSM/YSZ composite powder with appropriate amounts of terpeneol and ethyl cellulose. In each case, the ratio of solid content to organic content and also the ratio between terpeneol and ethyl cellulose was kept constant. The paste/ink was then applied onto one side of YSZ electrolyte

substrate using a brush, followed by firing at 1175°C per 2 h. To study the influence of electrolyte thickness on the parameters under study, L40/Y60, L60/Y40 and L70/Y30 cathodes were fabricated on thicker pellets also. Standard working electrode (WE) thus fabricated had an area of $\sim 0.75 \text{ cm}^2$ and $75 \mu\text{m}$ thickness. Care was taken to ensure that resulting cathode thickness in each case after firing is nearly identical. For L60/Y40 composition, cathodes with three different thicknesses (~ 50 , ~ 75 and $\sim 100 \mu\text{m}$) were fabricated. In addition, cathodes with three different areas (~ 0.5 , ~ 0.75 and $\sim 0.9 \text{ cm}^2$) were fabricated for L60/Y40 and $\sim 50 \mu\text{m}$ thick cathodes to study the influence of distance between WE and reference electrode (RE) on the parameters under study. Cross-sectional microstructure of the electrode/electrolyte interface was examined using the field emission scanning electron microscope (FESEM) (Carl Zeiss). LSM and YSZ phases in the cathode electrode were identified through EDX analysis.

Pt paste was painted symmetrically (equal to the cathode area onto the other side of the YSZ electrolyte) and as a ring concentrically to the WE and fired at 850°C to serve as counter electrode (CE) and RE, respectively. The gap between the WE and the ring RE was $\sim 4 \text{ mm}$ for the cathode with 0.75 cm^2 area and distance decreased with increase in the cathode area. Pt mesh was used as current collector for both working and counter electrodes. Pt paste was used to establish a bond between electrodes and the mesh (figure 2a and b). Cross-sectional SEM studies were also performed on the Pt layer along with the cathode to investigate the nature of the current collection layer and possible Pt infiltration into the cathode layer.

Electrochemical impedance spectroscopy (EIS) measurement of LSM and LSM/YSZ composite cathodes was conducted using an electrochemical instrument (CHI 604 2D electrochemical work station) under open circuit condition and in three electrode configuration (figure 2c). The frequency was swept from 1 MHz to 0.01 Hz with excitation amplitude of 10 mV. Impedance measurements were performed in air over a temperature range of 200 – 700°C . Cumulative ohmic resistance (electrolyte + electrodes) was obtained by performing the EIS in the two electrode configuration (figure 2d). All the impedance spectra were analysed and fitted using ZSimpWin Software. Though LSM/YSZ is a high temperature cathode material ($> 800^\circ\text{C}$), experiments were carried out only till 700°C due to our experimental limitations. However, it would not have any bearing on the conclusions drawn as temperature dependence of polarization resistance is higher than that of the Ohmic resistance and on increasing the temperature, polarization resistance can be expected to decrease to a greater level than that of the Ohmic resistance.

3. Results and discussion

XRD patterns (figure 3) of ball-milled L50/Y50 composite powder shows the broader peaks for YSZ when compared

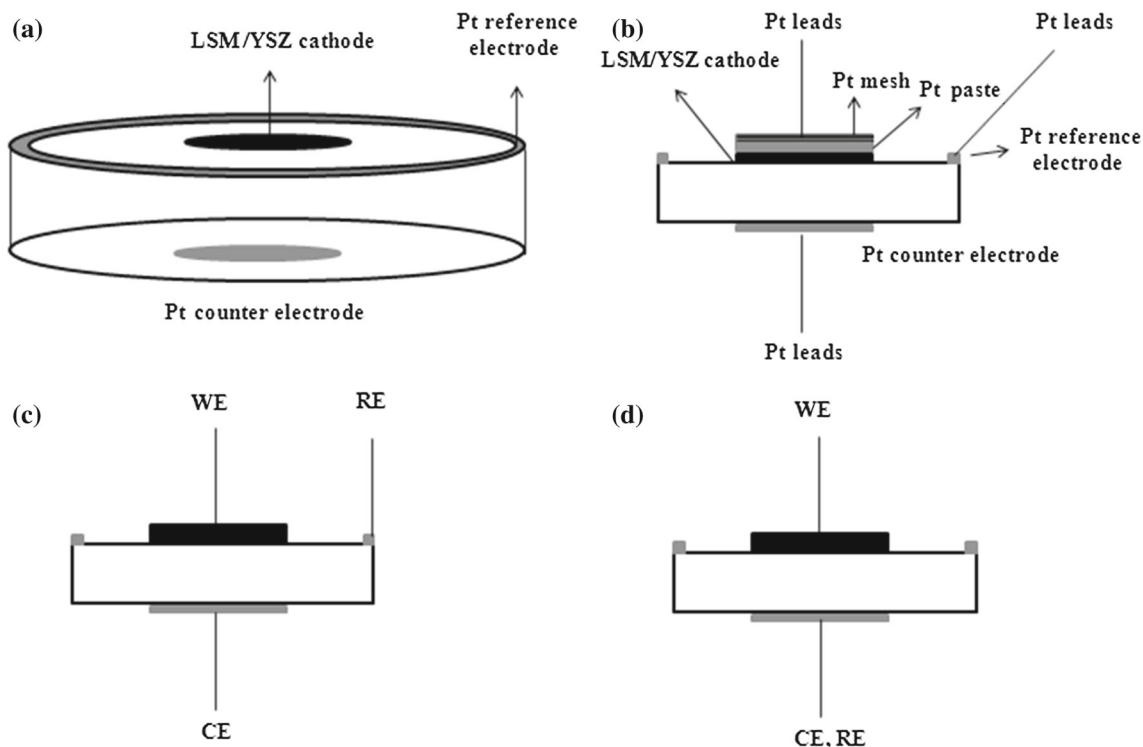


Figure 2. (a and b) Schematic representation of positioning of working, counter and reference electrodes. Configuration used for measuring the (c) cathode polarization and (d) cumulative ohmic resistance from the cathode and the electrolyte.

to LSM indicating the smaller crystallite sizes in YSZ powder. Particle size analysis studies suggest that average size of the particles in the ball-milled YSZ powder ($\sim 0.13 \mu\text{m}$) is smaller than the ball-milled LSM powders ($\sim 3 \mu\text{m}$) (figure 4a and b). Ball-milled composite powder (L50/Y50) showed a bimodal particle size distribution with particle size of $0.1 \mu\text{m}$ corresponding to YSZ and $3 \mu\text{m}$ corresponding to LSM.

Figure 5a and b shows the SEM micrograph showing the cross-sectional view of L100/Y0 and L50/Y50 composite cathode on the YSZ electrolyte and figure 5c shows the SEM micrograph of the Pt current collecting layer on the L100/Y0 cathode.

Pure LSM cathode shows many round-shaped particles with near point-to-point inter-particle unions (figure 5a). The individual nature of many particles ($\sim 3 \mu\text{m}$) is maintained at many regions even after firing. Face to face inter-particle unions could also be seen in some places. Pore size in the cathode is close to the particle size ($\sim 3 \mu\text{m}$). Closer examinations of the cathode/electrolyte interface (where TPB's are present) suggest the formation of face-to-face contacts between the cathode and the electrolyte.

The LSM and YSZ grains in the LSM/YSZ cathode appear to have adhered well with each other and bonded well at the LSM/YSZ-YSZ interface (figure 5b). Average thickness of the cathode in all the standard half cells was nearly equal ($\sim 50 \mu\text{m}$). Qualitatively, the amounts of LSM and YSZ appears to agree with the planned compositions (50:50),

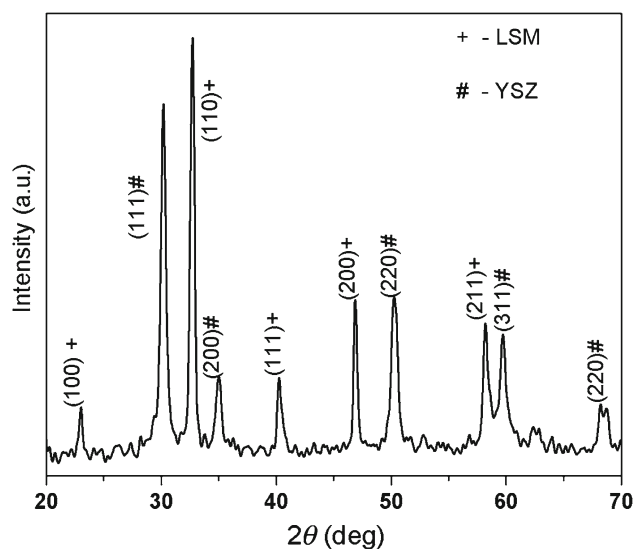


Figure 3. XRD pattern of ball-milled L50/Y50 composite powder.

while the amount of pore phase is approximately close to it in the case of pure LSM cathodes. Additionally, the LSM particle size appeared to be significantly larger than that of YSZ, in agreement with the larger average particle ($\sim 3.0 \mu\text{m}$) and crystallite size of the LSM in the starting powder when

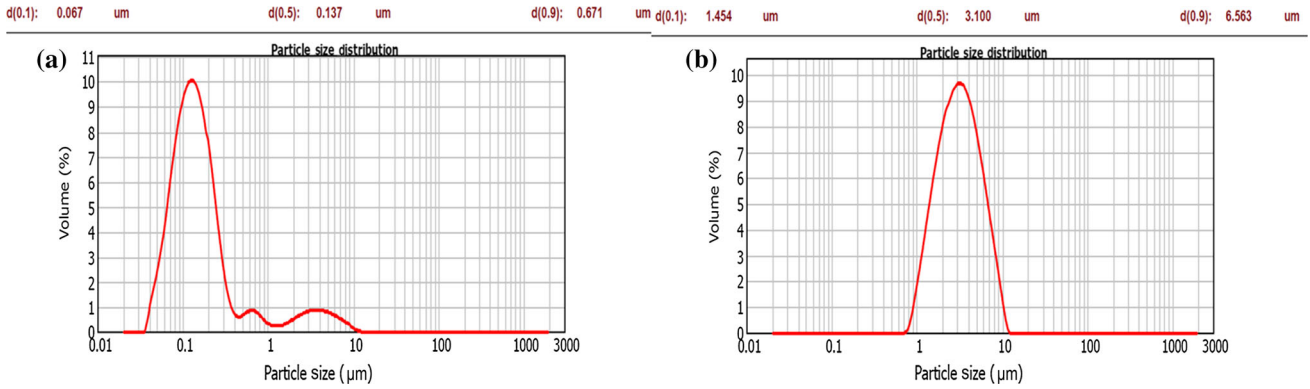


Figure 4. Particle size distribution in milled (a) YSZ and (b) LSM powders.

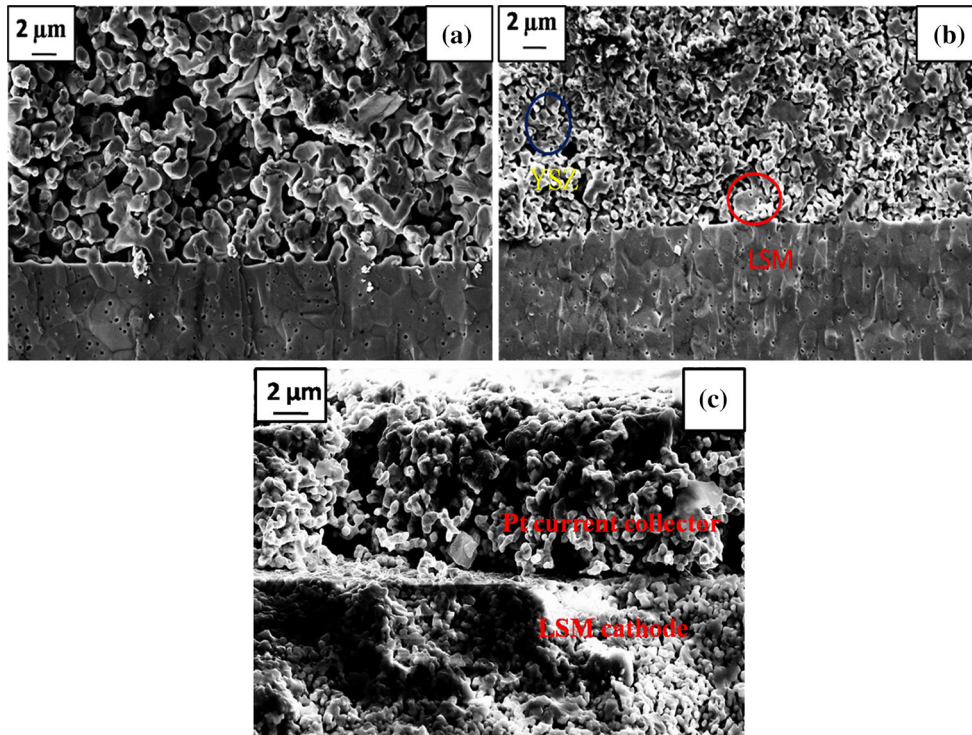


Figure 5. Cross-sectional SEM image showing the electrolyte/electrode interface with (a) LSM and (b) L50/Y50 composite as cathode. (c) Cross-sectional SEM image showing the Pt current collector and LSM cathode.

compared to the particle size ($\sim 0.15 \mu\text{m}$) in YSZ powder. Though porosity level in the composite cathode is lower than the LSM cathode, it would have a little effect on the conclusions drawn. Figure 5c clearly indicates that Pt has not diffused in to the cathode layer and hence would not influence the characteristics of the cathode. Pt layer is also porous enough to allow easy flow of gases.

Figure 6 shows a Nyquist plot illustrating the impedance response of L40/Y60 composite cathode measured in air at 700°C in the three electrode configuration. Impedance response from the three electrode EIS analysis would consist of cathode polarization and some un-compensated ohmic

resistances from the electrode and surface of the electrolyte. EIS response of the composite cathode is in accordance with the ones reported in the literature [11,21,22,33,34]. EIS data were fitted using an equivalent circuit (shown in the inset of figure 6) consisting of a series ohmic resistance (R_s), and two standard resistor-constant phase element ($R_{\text{HF}}(\text{CPE})_1$ and $R_{\text{LF}}(\text{CPE})_2$) by using Zsimpwin software. Here HF (high frequency) and LF (low frequency) are used to suggest the frequency regions of impedance response. A typical fit is shown in figure 6 and demonstrates a good agreement between experimental and the fitted curve. Sum of R_{HF} and R_{LF} gives the cathode R_p . Table 1 summarizes values

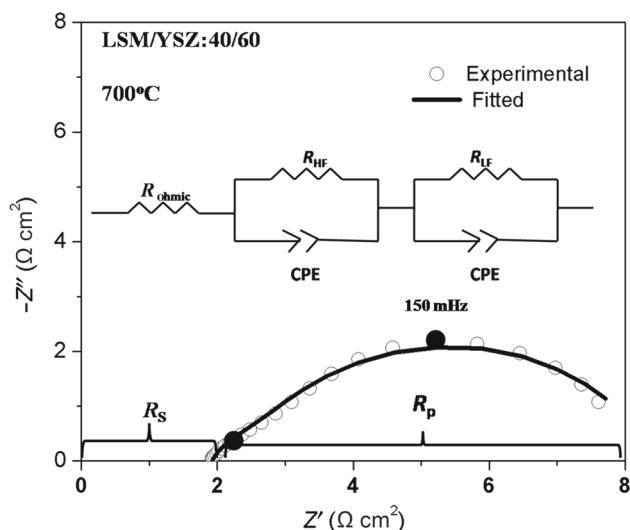


Figure 6. Fitting of EIS data (three electrodes) for L40/Y60 composite cathode at 700°C under OCV and the equivalent circuit used for fitting (inset).

obtained for different parameters on fitting EIS spectra to the equivalent circuit $R_s(R_{HF}(CPE)_1)(R_{LF}(CPE)_2)$. Two semicircles in the spectra could be due to any of the four steps mentioned in the figure 1 or the combination of them. Many inconsistencies with regard to the rate-limiting steps and associated activation energies for ORR can be seen in the literature. Activation energies in the range of 1.5–2.11 eV have been reported in the literature and surface processes ((i) and/or (ii)) are mostly considered as rate-determining steps [11,35–38].

In the literature, impedance spectra with either two or three semicircles have been reported for LSM/YSZ composite cathodes. For impedance spectra showing two semicircles, semicircle at high frequency has been attributed to the processes occurring at the TPB (step (iii)), whereas low-frequency responses have been attributed to the phenomenon occurring at regions within the electrode, farther away from the TPB. It is generally ascribed to the dissociative adsorption of oxygen (step (i) and/or (ii)). In the case of impedance spectra with three semicircles, the intermediate-frequency resistance (low frequency for a two arc spectra) has been correlated with the dissociative adsorption process. The third arc in the low frequency has been attributed to diffusion of O_2 or surface diffusion of O_{ad} . Some of the observations that were made with regard to the intermediate frequency

responses (in the case of three semicircles) are: (1) oxygen partial pressure has strong influence on it, (2) it is strongly dependent on the TPB density. Based on these observations, it was suggested that the intermediate-frequency resistance can be directly related to the TPB length and adjacent surface area of the phase facilitating dissociative adsorption [39–41]. Opposed to the intermediate frequency arc, high frequency arc has been reported to be independent of oxygen partial pressure. It has been associated with oxygen ion transport from LSM to YSZ in the electrode or from YSZ (electrode) to YSZ (electrolyte) or correlated with the movement of oxygen ions within YSZ grain boundaries of the composite cathode ((step (iii) and/or (iv)). There are conflicting reports with regard to the origin of high frequency semicircle. Table 2 summarizes some of the observations in the literature with regard to the rate-limiting steps, their dependence on the external variation and their associated activation energies for LSM/YSZ composite cathodes. L and W used in the equivalent circuit representation are respectively inductor and the warburg elements.

Few observations can be made while comparing the parameter values of our studies (table 1) with the literature information listed in table 2. Fitted values of the present study suggest that both the semicircles are associated with very high capacitance (in the order of mF). The capacitance value of the low frequency arc (in mF) is consistent with the high pseudo-capacitance values usually associated with adsorption and diffusion processes. As high frequency semicircle also exhibited the capacitance in the same order (in mF), it must also be associated with some electrochemical phenomenon.

For further analysis of the observations and for comparing it with the reported results, variation of each of the parameter of the equivalent circuit (R_s , R_{HF} , R_{LF} and $R_{HF} + R_{LF}$) was closely monitored as a function of temperature. The temperature dependences of all the resistances for L40/Y60 samples are illustrated in figure 7. All the processes exhibited an Arrhenius behaviour with temperature. Activation energy (~ 1.23 eV) of the R_{LF} , generally ascribed to the oxygen-dissociative process, is nearly in accordance with the reported literature value [21]. However, activation energy associated with R_{HF} (~ 2.5 eV) is much higher than the generally reported values in the literature [11,21,22,33]. Activation energies for grain and grain boundary O^{2-} ion conduction in YSZ would generally be in the range of ~ 0.7 and ~ 1.4 eV, respectively. Activation energy of ~ 0.7 eV for high frequency non-zero intercept resistance (R_s) suggests that it is related to

Table 1. Impedance parameters obtained for L40/Y60 composite cathodes at 700°C on fitting impedances spectra to equivalent circuit $R_s(R_{HF}(CPE)_1)(R_{LF}(CPE)_2)$.

R_s ($\Omega \text{ cm}^2$)	R_{HF} ($\Omega \text{ cm}^2$)	(CPE) ₁ , Y_0 (S.s ⁿ)	Freq. power n_1	f_r (Hz)	R_{LF} ($\Omega \text{ cm}^2$)	(CPE) ₂ (S.s ⁿ)	n	f_r (Hz)	R_p ($\Omega \text{ cm}^2$)
1.92	0.62	0.13	0.76	~ 0.15	5.91	0.20	0.77	~ 50	6.53

Table 2. Literature summary of the EIS response for LSM/YSZ composite cathode, equivalent circuit used for the analysis of the spectra, observation with regard to the responses at the different frequency domains and corresponding activation energy.

Details about the cathode composition, cathode firing temperature, experimental conditions	Number of semicircles and the equivalent circuit used	R_{HF} observation/comments, activation energy, conclusions	R_{MF} observation/comments, activation energy, conclusions	R_{LF} observations/comments, activation energy, conclusions	Ref.
LSM50/YSZ50, 1075–1375°C, 800°C, Varying P_{O_2}	Two, LRs(R_{HF} (CPE)) (R_{LF} (CPE))	Negligible dependence on P_{O_2} , R_{HF} decreases with increase in firing temperature $E_a \sim 1$ eV, O^{2-} conduction in YSZ of electrode	—	Strong P_{O_2} dependence, shows a minimum R_{LF} at intermediate firing temperature, 1.6 eV, adsorption and charge transfer mechanism	[22]
LSM50/YSZ50, varying particle size between LSM an YSZ, 1175°C, 600–900°C, variable dc polarization	Three, LRs(R_{HF} (CPE)) (R_{MF} (CPE)) (R_{LF} (CPE))	R_{HF} decreasing under polarization, attributed to activation of LSM and conversion into MEIC, $E_a \sim 0.9$ eV, O^{2-} conduction in YSZ of electrode	R_{MF} was lower for LSM and YSZ with smaller particle size, strongly depends on the TPB, oxygen dissociative process, $E_a \sim 1.25$ eV	Oxygen surface diffusion	[21]
LSM50/YSZ50, 1100°C	Two, LRs (R_{HF} (W))(R_{LF} (CPE))	R_{HF} increases with thickness of cathode, $E_a \sim 1.05$ eV, originates from grain boundary of YSZ	—	Depends on the partial pressure of O_2 , $E_a \sim 1.5$ eV	[11]
LSM50/YSZ50, 1150°C, varying the cathode thickness 650°C, $P_{O_2} = 0.21$ atm	Two, R_s (R_{HF} (CPE), (R_{LF} (CPE))	$C \sim 2$ mF cm ⁻² , $E_a \sim 0.76$ eV, O^{2-} conduction in YSZ	—	$C \sim 18$ – 32 mF cm ⁻² , $E_a \sim 2.09$ eV, adsorption and diffusion processes	[33]
Dense thin film of LSM microelectrodes on the YSZ thin film	$R_s W$ (R_{HF} (CPE), (R_{LF} (CPE))	$C \sim 3.2 - 10^{-3}$ F cm ² , $E_a \sim 2.42 - 3.05$ eV, charge transfer at TPB or participation of bulk of LSM in ORR	—	$C \sim 3.4 \times 10^{-4}$ F cm ² , $E_a \sim 1.71 - 1.88$ eV, adsorption and diffusion processes	[17]

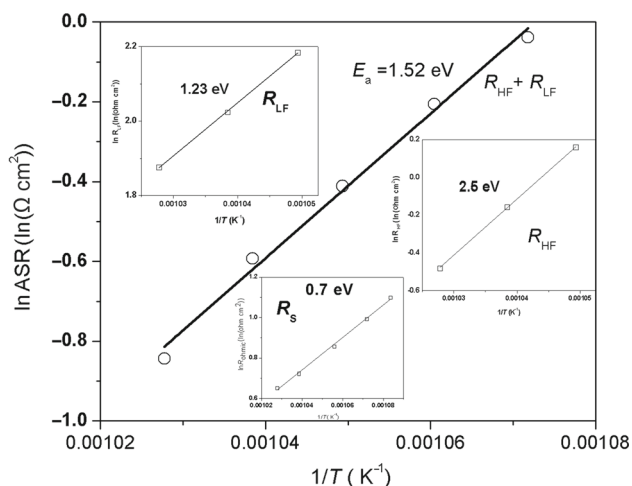


Figure 7. Temperature dependence of polarization resistance ($R_{HF} + L_{HF}$), high-frequency response resistance (R_{HF}), low-frequency response resistance (L_{HF}) and series resistance (R_s) for L40/Y60 composite cathodes.

the O^{2-} ion conduction in YSZ lattice of electrode and partly in the electrolyte. Since observed activation energy for high-frequency phenomenon (~ 2.5 eV) is not close to either grain (~ 0.7 eV) or grain boundary (~ 1.4 eV) and capacitance (mF) also being much higher than generally associated with either of them ($C_g \sim 10^{-10}$ F, $C_{gb} \sim 10^{-7}$ to 10^{-8} F) [34], it would be improper to link the high-frequency phenomenon (R_{HF}) to the O^{2-} ion conduction in the YSZ. We believe that in the temperature range of investigation (650 – 750°C), the response for O^{2-} conduction in the YSZ regions of electrode and actual electrolyte lie above the maximum frequency employed for the impedance analysis. Though more investigations are required to ascertain its origin and characteristics, we are bound to believe that high-frequency response (R_{HF}) has the origin other than the grain/grain boundary ion conduction and mostly emanates due to some electrochemical mechanism at the TPB.

Our observations are close to the ones reported by Jiang *et al* [33] and La *et al* [17]. La *et al* [17] studied the ORR on the patterned, dense thin film LSM microelectrodes on the YSZ thin film systems. As in our case, Nyquist plots of those LSM microelectrodes around 700°C consisted of two distinct semicircles with non-zero intercept at high frequency. High-frequency non-zero intercept with average activation energy of 1.16 eV was attributed to ion transport in YSZ thin film. Low-frequency semicircle with activation energies in the range 1.71 – 1.88 eV and an average capacitance value of $\sim 3.4 \times 10^{-4}$ F cm^{-2} was attributed to surface process. Interestingly, parameters associated with high-frequency semicircles ($E_a \sim 2.42$ – 3.05 eV and $C \sim 3.2$ – 10^{-3} F cm^{-2}) were strikingly similar to the values that we observed. They attributed the high frequency phenomenon to charge transfer mechanism occurring at TPB and/or to bulk of LSM participating in ORR reaction due to LSM becoming mixed

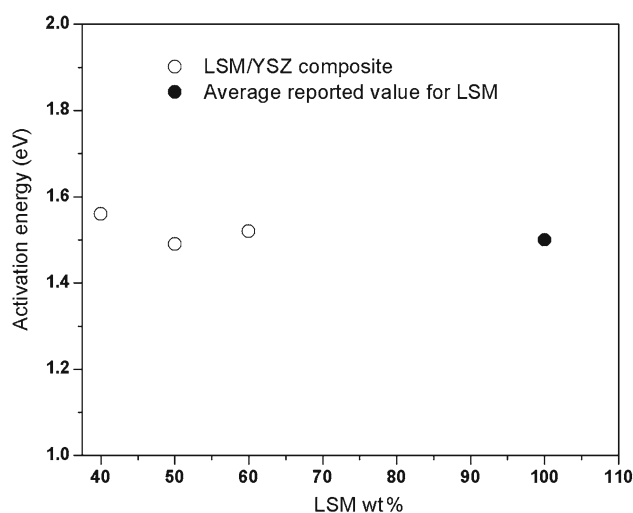


Figure 8. Variation of activation energy of polarization resistance with composition for LSM/YSZ composite cathode.

ionic and electronic conductor (MEIC). They based their argument to the (1) similarity between their observed activation energy to the reported activation energy (2.6 – 3.0 eV) for bulk oxide ion transport processes in LSM [8,42] (based on tracer diffusion measurements) and (2) high capacitance (1×10^{-1} F cm^{-2}) associated for MEIC $\text{La}_{1-x}\text{Sr}_x\text{O}_{3-\delta}$ where oxygen reduction via the bulk pathway dominates [43,44]. High capacitance ($\sim 10^{-3}$ F cm^{-2}) was also observed for dense thin films of LSM, where oxygen reduction via bulk pathway dominated [45]. These observations prompt us to attribute the high-frequency semicircle to some electrochemical phenomenon and not to the ion conduction in the YSZ lattice.

Figure 8 shows the variation in the activation energy of the R_p ($R_{HF} + R_{LF}$) of the composite cathode with the composition. Near constancy of overall activation energy (~ 1.5 eV) probably suggest that two mechanisms, corresponding to high- and low-frequencies are interlinked and their resistance increase/decrease proportionately with the composition and thereby keeping the overall activation energy constant. Hence, high frequency semicircle must also be emanating as a consequence of some electrochemical phenomenon.

Figure 9 shows a Nyquist plot illustrating the impedance response of all the cathode samples measured in air at 700°C . For easy comparison, uncompensated ohmic contribution was subtracted from the each impedance response and spectra were fitted to the equivalent circuit (RQ)(RQ). Solid lines in the impedance spectra (fitted curve) clearly suggests that equivalent circuit fits well to the impedance spectra of all the cathodes and fitted parameters are summarized in table 3. Polarization ASR (R_p) decreases with increasing YSZ content to a minimum at 40 wt% of YSZ, after which the resistance again increases (figure 10a). Observations from the present study are slightly different from some of the reported trends. Studies have shown minimum R_p value for 50 wt% YSZ with

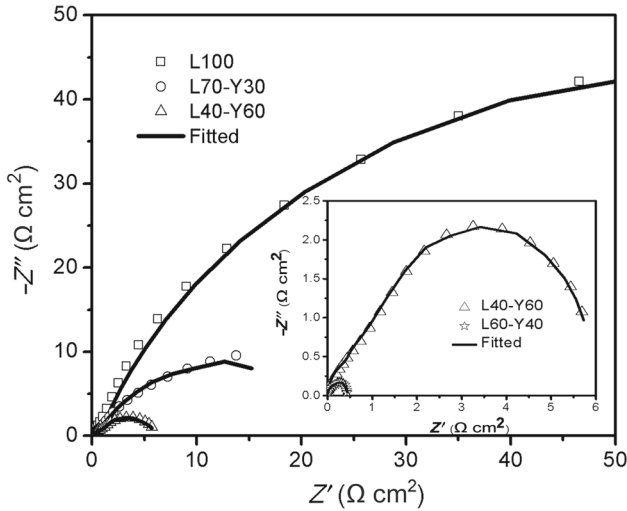


Figure 9. Nyquist plot of the impedance responses for all the cathode compositions measured at 700°C under OCV conditions. Solid line is the fitted curve.

resistances increasing quite symmetrically on either side of this composition [14]. However, minimum at 50 wt% can be expected only when density of LSM and YSZ are same and particle sizes are equal. Since the density of LSM (6.5 g cm^{-3}) is slightly higher than YSZ (6.05 g cm^{-3}) and LSM with 25 times larger particle size than YSZ was used in the present study, the occurrence of minimum polarization at higher composition of LSM value is not unexpected. If only R_p values are considered, L60/Y40 composites are ideal due to their low values ($R_p \sim 0.5 \Omega \text{ cm}^2$). However, it is also essential to know the ohmic resistance from the L60/Y40 cathode and its magnitude in comparison to the other compositions, before concluding that L60/Y40 is the best composition.

High-frequency non-zero intercept of the Nyquist plot obtained from the EIS studies of the cell in the two electrode configuration (figure 2b and d) would consist of total ohmic resistance (electrode + electrolyte). Two electrode EIS was performed on all the samples at 700°C and OCV conditions and total ohmic resistance was noted from the high-frequency intercept.

Resistivity obtained for the YSZ electrolyte with LSM electrode was considered as a reference value ($\rho_{\text{LSM}}(\text{YSZ})$).

Table 3. Impedance parameters obtained for composite cathodes at 700°C on fitting impedances spectra to equivalent circuit ($R_{\text{HF}}(\text{CPE})_1)(R_{\text{LF}}(\text{CPE})_2$).

Sample	R_{HF} ($\Omega \text{ cm}^2$)	CPE_1 , Y_0 (S.s^n)	Freq. power, n_1	R_{LF} ($\Omega \text{ cm}^2$)	CPE_2 , Y_0 (S.s^n)	Freq. power, n_2	Total R_p ($\Omega \text{ cm}^2$)
L100	0.64	0.18	0.8	118.4	0.036	0.80	119.0
L70-Y30	0.72	0.16	0.89	23.64	0.27	0.78	24.35
L60-Y40	0.24	2.63	0.95	0.19	0.67	0.98	0.43
L40-Y60	0.62	0.13	0.76	5.91	0.20	0.77	6.53

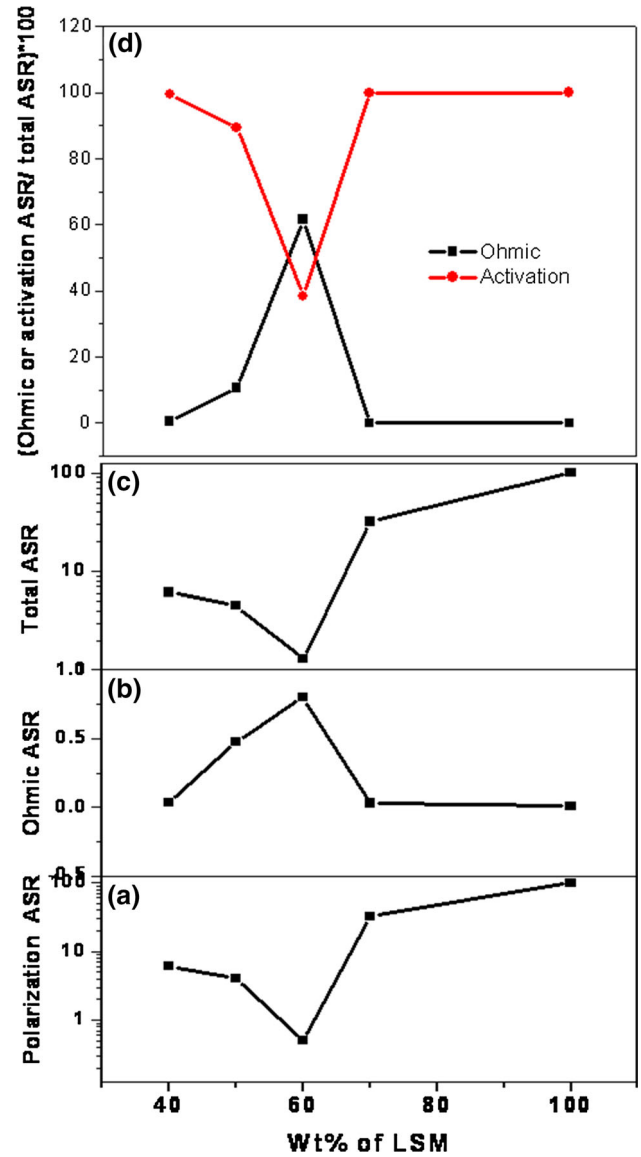


Figure 10. Variation of (a) polarization, (b) ohmic and (c) total ASR at 700°C for LSM/YSZ composite with different compositions. (d) Percentage of contribution from ohmic and polarization resistance to the overall resistance.

$$\rho_{\text{LSM}}(\text{YSZ}) = (R \times A)/L, \quad (1)$$

where L is the thickness of the electrolyte and A the area of the LSM cathode used.

In all the cases, platinum (Pt) was used as a counter electrode and it was assumed that Pt electrode does not contribute to the ohmic resistance. Hence, the additional component of the total ohmic resistance obtained while performing EIS on LSM/YSZ composite can be assumed to be originating due to the cathode electrode. Additional ohmic resistance ($R_{\text{cathode(ohmic)}}$), while using composite cathode was calculated using the following equation.

$$R_{\text{cathode(ohmic)}} = R_{\text{obs(ohmic)}} - (\rho_{\text{LSM(YSZ)}} \times L_1/A_1), \quad (2)$$

where $R_{\text{obs(ohmic)}}$ is the total ohmic resistance measured with a given composite cathode. L_1 and A_1 are the thickness of the electrolyte and area of the LSM/YSZ composite cathode. Thickness of the electrolyte used for the each of the composite cathode and the area of the cathode in each case were measured accurately to avoid any errors in the resistance measurements. Maximum care was taken to keep the contact resistance and lead resistance minimal (even if they are present, they would be same for all samples, as identical experimental method was used in each case). $R_{\text{cathode(ohmic)}}$ (R_{ohmic}) thus obtained for different compositions is shown in figure 10b. As per equation 2, R_{ohmic} for pure LSM is zero. Total resistance from cathode ($R_{\text{Ohm}} + R_p$) is shown in figure 10c.

R_{ohmic} that was observed on using L70/Y30 composite cathode was very low. High R_p and low R_{ohmic} observed in the case of L70/Y30 suggest that most of the electrochemical reactions in the L70/Y30 cathode is confined mostly to the electrolyte/electrode interface. Added YSZ is not high enough to form a percolated network through the bulk of the cathode and hence, does not participate in the formation of additional electrochemically active TPB's (EATPB). Even if they are formed, they are very limited in number. Small decrement in the R_p for L70/Y30 when compared to L100 indeed suggests the same. On further increasing the YSZ content to 40%, R_p decreases dramatically ($0.43 \Omega \text{ cm}^2$) along with significant increase in the R_{ohmic} ($0.7 \Omega \text{ cm}^2$). Decreased R_p suggests the participation of increased number of TPB's from the cathode. Increased number of O^{2-} ions thus generated in the cathode has to travel through the YSZ component of the cathode, which has been sintered only at 1200°C ; much lower than the sintering temperature required for its complete densification. Even if the distance that ions need to travel in cathode (maximum $\sim 50 \mu\text{m}$) is shorter when compared to distance it travels in the electrolyte ($\sim 300 \mu\text{m}$), chances of O^{2-} encountering high resistive grain boundaries/interfaces is much higher in such a cathode, while comparing to dense electrolyte. Hence, relative ohmic contribution of the cathode can be expected to be disproportionately higher corresponding to its thickness.

Contrary to the general observation during electrical measurements that ohmic resistance increases with increase in the amount of YSZ, we observed a decrease in the R_{ohmic} , while increasing the wt% of YSZ to 50 and then to 60%. Perception would be indeed correct, if electrical conductivity measurements are carried out on the LSM/YSZ composite cathode.

Since electrical conductivity of YSZ is 4 orders of magnitude smaller than the electrical conductivity of LSM, overall electrical conductivity would decrease with increase in the amount of YSZ. However, when it performs the role of cathode, as in the present case, overall resistance of a charge would be the sum of resistances it faces while travelling as an e' current (in LSM) and the resistances it faces while travelling as O^{2-} current (in YSZ) after the conversion of e' current into O^{2-} current at TPB (figure 1b). Overall resistance in such a case would be dictated by the relative distance it travels as an e' current and O^{2-} current.

During such a travel, majority of ohmic loss would occur while travelling via YSZ due to the higher electrical resistance. Resistance would be lower if broader paths are available for the O^{2-} ions that are created at the TPB, which would be the case with higher volume fraction of YSZ. It was observed in the composition range that we investigated. Both R_p and R_{ohmic} can be expected to increase on further increase in the YSZ ($>70 \text{ wt\%}$ of YSZ) component due to the isolation of LSM phase. At L60/Y40, where minimum R_p was observed, R_{ohmic} constituted about 60% of overall resistance (figure 10d). Nonetheless, overall resistance is still lowest for the L60/Y40 composition (figure 10c). Effect of the composition is more pronounced on the number of TPB's and in turn on the R_p when compared to the effect on R_p . Despite of higher R_p , L60/Y40 is preferred over other composites because of the lower total resistance. Similar results were observed while conducting the experiment by using the thicker electrolytes. With increase in the cathode thickness, ohmic resistance increased.

In the electrolyte supported cell (as in the present case), where the thickness of cathode is only about 15% of the overall thickness, R_{ohmic} contribution from cathodes amounts to about 25–30% total ohmic resistance, while opting for the composite cathode. However, R_{ohmic} gets masked due to the significant decrease in the R_p . Hence, the additional R_{ohmic} from the composite cathode goes unnoticed in the electrolyte supported cells. However, in the anode supported cell, where the thickness of the electrolyte is generally $<20 \mu\text{m}$, R_{ohmic} from the composite cathode can even be higher than the ohmic resistance from the electrolyte itself. Moreover, it can be expected that with decrease in the electrolyte resistance (with decrease in the electrolyte thickness), R_p of pure LSM will decrease significantly due to the increase in the conductance of the electrolyte. However, R_{ohmic} contribution from cathode would remain unchanged and would contribute significantly. It would be interesting to see whether overall resistance of composite cathode is lower than that of pure LSM cathode even in the case of anode-supported cells, where the thickness of the electrolyte is very low. It can be conjectured that performance of LSM/YSZ composite cathode may not be much superior than that of plain LSM in the case of anode-supported SOFC with thin electrolyte. Experiments are underway to ascertain the same. It would also be interesting to see the magnitude of ohmic resistance contribution in the case of nano-structured impregnated cathodes of LSM/YSZ, in

which nano-sized LSM of varied quantity are generally formed in the dense skeleton of YSZ through impregnation process. Investigations are underway in discerning and quantifying the ohmic contribution in the impregnated cathodes and comparing it with conventional LSM/YSZ composite cathodes.

4. Conclusions

Performance of the LSM/YSZ composite cathode was evaluated by measuring the overall resistance from the cathode by varying its composition. Isolation of ohmic and polarization contribution to the overall cathode resistance was done by performing EIS in two and three electrode configurations. Like polarization resistance, even ohmic resistance was found to be dependent on the composition of the cathode, though to a lesser extent. LSM/YSZ composite with 60:40 weight ratios was found to be ideal due to overall low polarization ($\sim 2.49 \Omega \text{ cm}^2$). Polarization resistance was also lowest at the same composition ($\sim 0.49 \Omega \text{ cm}^2$). However, ohmic polarization was highest for this cathode ($\sim 2 \Omega \text{ cm}^2$) and constituted about 75% of the overall resistance. Compositional dependence of polarization and ohmic resistance were explained based on the variation in the number of TPB's and the ease with each O^{2-} ions formed at the TPB's can move into the electrolyte through the YSZ component of the electrode. For electrolyte-supported cells, ohmic contribution from electrodes may go unnoticed due to the dominance of electrolyte ohmic resistance. However, in anode-supported cells with thin electrolyte ($< 10 \mu\text{m}$), ohmic contribution from composite electrodes might amount to a significant proportion or might even surpass the ohmic contribution from real electrolyte ohmic resistance. In such a scenario, it needs to be ascertained whether decreased polarization resistance through the increase in the number of TPB's indeed compensates for the increase in the ohmic resistance, while using LSM/YSZ composites. Studies are underway to check the superiority of LSM/YSZ composite over LSM and its magnitude in anode-supported SOFC with thin electrolyte.

Acknowledgements

We acknowledge CSIR, ESC-01-04 for funding the project. We also thank the director, NAL-CSIR and the head, SED for the encouragement. Help received from Mr Srinivas, Mr Balaji and Mr Siju in carrying out XRD, particle size and FESEM analysis is also appreciated.

References

- [1] De Souza S, Visco S J and De Jonghe L C 1997 *J. Electrochem. Soc.* **144** L35
- [2] Kim S D, Hyun S H, Moon J, Kim J H and Song R H 2005 *J. Power Sources* **139** 67
- [3] Will J, Mitterdorfer A, Kleinlogel C, Perednis D and Gauckler L J 2000 *Solid State Ionics* **131** 79
- [4] Xu X, Xia C, Huang S and Peng D 2005 *Ceram. Int.* **31** 1061
- [5] Jiang S P 2003 *J. Power Sources* **124** 390
- [6] Ji Y, Kilner J A and Carolan M F 2005 *Solid State Ionics* **176** 937
- [7] Steele B C H 1995 *Solid State Ionics* **75** 157
- [8] Yasuda I, Ogasawara K, Hishinuma M, Kawada T and Dokiya M 1996 *Solid State Ionics* **86–88** 1197
- [9] Smith J R, Chen A, Gostovic D, Hickey D, Kundinger D, Duncan K L *et al* 2009 *Solid State Ionics* **180** 90
- [10] Fukunaga H, Ihara M, Sakaki K and Yamada K 1996 *Solid State Ionics* **86–88** 1179
- [11] Murray E P, Tsai T and Barnett S A 1998 *Solid State Ionics* **110** 235
- [12] Østergård M J L, Clausen C, Bagger C and Mogensen M 1995 *Electrochim. Acta* **40** 1971
- [13] Wilson J R, Duong A T, Gameiro M, Chen H Y, Thornton K, Mumm D R *et al* 2009 *Electrochem. Commun.* **11** 1052
- [14] Wilson J R, Cronin J S, Duong A T, Rukes S, Chen H Y, Thornton K *et al* 2010 *J. Power Sources* **195** 1829
- [15] Chen K, Ai N and Jiang S P 2012 *Int. J. Hydrogen Energy* **37** 1301
- [16] Wu L, Jiang Z, Wang S and Xia C 2013 *Int. J. Hydrogen Energy* **38** 2398
- [17] La O G J, Yildiz B, McEuen S and Shao-Horn Y 2007 *J. Electrochem. Soc.* **154** B427
- [18] Roy A S, Gupta S, Seethamraju S, Madras G and Ramamurthy P C 2014 *Composites Part B: Engineering* **58** 134
- [19] Roy A S, Gupta S, Seethamraju S, Ramamurthy P C and Madras G 2014 *Sci. Adv. Mater.* **6** 946
- [20] Roy A S, Saravanan S, Kishore, Ramamurthy P C and Madras G 2014 *Polym. Compos.* **35** 1636
- [21] Duong A T and Mummz D R 2012 *J. Electrochem. Soc.* **159** B39
- [22] Cronin J S, Muangnapoh K, Patterson Z, Yakal-Kremiski K J, Dravid V P and Barnett S A 2012 *J. Electrochem. Soc.* **159** B385
- [23] Kenney B, Valdmanis M, Baker C, Pharoah J G and Karan K 2009 *J. Power Sources* **189** 1051
- [24] Abbaspour A, Nandakumar K, Luo J and Chuang K T 2006 *J. Power Sources* **161** 965
- [25] Chen D, Lin Z, Zhu H and Kee R J 2009 *J. Power Sources* **191** 240
- [26] Chen X J, Chan S H and Khor K A 2004 *Electrochim. Acta* **49** 1851
- [27] Zhang Y, Wang Y, Chen F and Xia C 2011 *J. Power Sources* **196** 1983
- [28] Shearing P R, Brett D J L and Brandon N P 2010 *Int. Mater. Rev.* **55** 347
- [29] Cronin J S, Chen-Wiegart Y-C K, Wang J and Barnett S A 2013 *J. Power Sources* **233** 174
- [30] Haanappel V A C, Mertens J, Rutenbeck D, Tropartz C, Herzhof W, Sebold D *et al* 2005 *J. Power Sources* **141** 216
- [31] Zhao F and Virkar A V 2005 *J. Power Sources* **141** 79
- [32] Yamahara K, Sholklapper T Z, Jacobson C P, Visco S J and De Jonghe L C 2005 *Solid State Ionics* **176** 1359
- [33] Jiang S P, Love J G and Ramprakash Y 2002 *J. Power Sources* **110** 201

- [34] Nielsen J and Hjelm J 2014 *Electrochim. Acta* **115** 31
- [35] Chen X J, Khor K A and Chan S H 2003 *J. Power Sources* **123** 17
- [36] Jørgensen M J and Mogensen M 2001 *J. Electrochem. Soc.* **148** A433
- [37] Siebert E, Hammouche A and Kleitz M 1995 *Electrochim. Acta* **40** 1741
- [38] Van Herle J, McEvoy A J and Ravindranathan Thampi K 1996 *Electrochim. Acta* **41** 1447
- [39] Song H S, Lee S, Hyun S H, Kim J and Moon J 2009 *J. Power Sources* **187** 25
- [40] Song H S, Kim W H, Hyun S H, Moon J, Kim J and Lee H W 2007 *J. Power Sources* 167 258.
- [41] Song H S, Kim W H, Hyun S H and Moon J 2006 *J. Electroceram.* **17** 759
- [42] De Souza R A, Kilner J A and Walker J F 2000 *Mater. Lett.* **43** 43
- [43] Adler S B 1998 *Solid State Ionics* **111** 125
- [44] Kawada T, Suzuki J, Sase M, Kaimai A, Yashiro K, Nigara Y et al 2002 *J. Electrochem. Soc.* **149** E252
- [45] Ioroi T, Hara T, Uchimoto Y, Ogumi Z and Takehara Z I 1998 *J. Electrochem. Soc.* **145** 1999